IEEE Access
Multidisciplinary | Rapid Review | Open Access Journal

Received December 31, 2020, accepted January 3, 2021, date of publication January 8, 2021, date of current version January 19, 2021.

Digital Object Identifier 10.1109/ACCESS.2021.3050167

Optimal Tracking Current Control of Switched Reluctance Motor Drives Using Reinforcement Q-Learning Scheduling

HAMAD ALHARKAN[1,2], (Student Member, IEEE), SEPEHR SAADATMAND[1], (Student Member, IEEE), MEHDI FERDOWSI[1], (Member, IEEE), AND POURYA SHAMSI[1], (Senior Member, IEEE)

[1]Electrical Engineering Department, Missouri University of Science and Technology, Rolla, MO 65401, USA
[2]Department of Electrical Engineering, College of Engineering, Qassim University, Unaizah 56452, Saudi Arabia

Corresponding author: Hamad Alharkan (haahx9@mst.edu)

ABSTRACT In this article, a novel Q-learning scheduling method for the current controller of a switched reluctance motor (SRM) drive is investigated. The Q-learning algorithm is a class of reinforcement learning approaches that can find the best forward-in-time solution of a linear control problem. An augmented system is constructed based on the reference current signal and the SRM model to allow for solving the algebraic Riccati equation of the current-tracking problem. This article introduces a new scheduled-Q-learning algorithm that utilizes a table of Q-cores that lies on the nonlinear surface of an SRM model without involving any information about the model parameters to track the reference current trajectory by scheduling the infinite horizon linear quadratic trackers (LQT) handled by Q-learning algorithms. Additionally, a linear interpolation algorithm is proposed to improve the transition of the LQT between trained Q-cores to ensure a smooth response as state variables evolve on the nonlinear surface of the model. Lastly, simulation and experimental results are provided to validate the effectiveness of the proposed control scheme.

INDEX TERMS Adaptive dynamic programming, current control, least square methods, motor drive, optimal control, reinforcement learning, switched reluctance motors.

I. INTRODUCTION

Lately, switched reluctance motor (SRM) has earned significant consideration for a wide range of transportation electrification and variable speed applications. This is because it has several inherences, such as a resilient and simple structure due to the lack of magnet, brushes, and rotor winding. Moreover, SRMs are efficient at high speed [1]. Based on the reduction in the power electronics costs, improved availability and performance of film capacitors to handle the pulse-type current of these machines, and the interest in the reduced utilization of rare-earth magnets, the utilization of SRMs for a variety of industrial and commercial applications has been on the rise [2]. This includes applications in traction drives as well as aeronautics where the high reliability, high temperature and vibration tolerance, and high-speed range of SRMs make them very competitive compared to more complex motors [3]–[7]. However, SRMs have suffered from certain drawbacks, including high acoustic noise production due to its torque ripple and flux paths and the expensiveness of drive due to a large number of semiconductor switches in its drive. Additionally, it has a highly nonlinear electromagnetic nature that is highly reliant on variations in the phase current and rotor positions. Many researchers have investigated SRMs to mitigate these issues by improving the SRM design to minimize torque ripples or developing a new converter topology using recently introduced and more affordable power electronics switches [8]–[11]. The highly nonlinear behavior of SRMs is the main challenge, which must be considered when designing an effective controller.

Unlike conventional sinusoidal motors, SRMs require pulse-type current that requires high variations of current (i.e. di/dt) and hence a high bandwidth drive system. To achieve a fast rate of current charge and discharge, a large dc-link voltage and low phase inductances are often needed. However, this dc-link voltage will make the regulation of phase currents more challenging, particularly during low speed operation modes. Traditionally, delta modulation or hystere-

The associate editor coordinating the review of this manuscript and approving it for publication was Ton Duc Do.

sis current controllers have been used to regulate the phase current. Hysteresis-type controllers lead to a variable switching frequency, which is not of interest as managing the Electro-Magnetic Interferences (EMIs) becomes challenging. Additionally, power switches will impose an upper limit for the switching frequency and large current ripples will increase torque ripple and audible noises.

Many publications have investigated current control techniques for SRM, including enhanced hysteresis control, sliding-mode approaches, and fast PI controllers [12]–[17]. However, PI-based methods are slow, and methods such as delta-modulation will not be able to use the concept of duty-cycle to breakdown the switching cycle to shorter active periods. Therefore, a method is required to generate a duty cycle. Classical controllers such as PID controllers are not capable of controlling a system with such transients. Hence, researchers have investigated methods such as model predictive control and neural networks to cope with this issue [18]–[23]. To cope with the nonlinearities of the model, Ref [19] has introduced a Taylor expansion algorithm to approximate the variations of the model as a function of the rotor angle and current. Also, adaptive estimators are used to improving this approximation. However, the accuracy of the control is impacted by the Taylor expansion. As an improvement, Ref [24] has introduced a table-based inductance function that is used to form the model needed for the Model Predictive Control (MPC) in each cycle as oppose to a Taylor expansion. This table allows the MPC to have access to an accurate inductance value for a given rotor angle and current. Additionally, an adaptive estimator is used to update this table. Ref [24] has also introduced a linear interpolation technique for transitions between the models that will be incorporated in this article to introduce a novel scheduled Q-learning technique. In these literatures, a fundamental model is assumed, then an adaptive estimator is used to estimate the inductance of the phase as a function of rotor angle and current. Then, this value is used in a model predictive controller. The main drawbacks of the above works are the need for a separate estimator, a model predictive controller, and assumptions on the structure of the model.

In this article, the controller has been formulated based on an infinite-horizon linear quadratic tracker (LQT). To eliminate the need for a known model, a reinforcement Q-learning scheme is used to learn and apply the best course of action at each control cycle. Q-learning is inherently a linear controller [25], and on the other hand, the model of an SRM has nonlinearities to rotor angle and current (i.e. saturation). Hence, this article proposes a scheduled Q-learning algorithm that utilizes a table of Q cores, each containing a linear controller for a given rotor angle and current. By transitioning between these Q cores using a linear interpolation mechanism, this article introduces a nonlinear tracking controller capable of handling SRM drives.

The specific contributions of this article include i) introduction of Q-learning LQT for SRMs, ii) scheduling a table of Q-cores to achieve nonlinear control capabilities out of traditional Q-learning techniques, and iii) introducing a linear interpolation technique for transitioning between Q-cores to achieve a smooth Q scheduling.

The article is organized as follows: Section II reviews the Q-learning algorithm and introduces the proposed controller. Section III proposes the Q scheduling algorithm and table interpolation. Sections IV and V verify the effectiveness of the proposed controller through simulations and experimental results.

II. Q-LEARNING CONTROL OF SRM DRIVE

As discussed in Section I, there are several approaches to current control SRMs with their own drawbacks. For instance, the hysteresis technique downside is its rippled current, and torque, and consequently the acoustic noises and low efficiency. The conventional linear controllers such as PI/PID lack the ability to cope with nonlinear systems. The nonlinear techniques such as model predictive controller rely on an accurate system model, which can be changed during the time. Therefore, model-free reinforcement learning is a powerful tool to tackle all these drawbacks. Considering the expensive computation costs for neural network-based reinforcement learning such as online adaptive optimal control problem of a class of continuous-time Markov jump linear systems (MJLSs) [26] or Online policy iterative-based H∞ optimization algorithm [27], it is infeasible to implement them into power electronics control circuits. On the other hand, the Q-learning technique based on the Q-table only requires enough memory spaces that are available in most of the power electronics microcontrollers.

The primary target of the Q-learning algorithm in the current control of SRMs is to solve the LQT problem, which allows the system output to track a specific reference signal. The implementation of the algorithm in this format minimizes the predetermined value function associated with the cost of the policy and the difference between the output current and the reference signal. The classic solutions to the LQT can be found by solving the feedback part using the algebraic Riccati equation (ARE) and a feedforward part using the noncausal difference equation [28]. However, these approaches are not applicable for SRMs or most of the industrial applications since they are solved offline and they need accurate information on system dynamics. Adaptive dynamic programming is a part of the Reinforcement Learning (RL) methods and has been used to solve infinite-horizon LQT problems online without knowing system dynamics [29]. Two major assumptions have been made for this scheme: full state feedback is observable for the controller and the full reference trajectory is known. The LQT is a special case of model predictive controllers were the performance index is quadratic and no further constraints are applied to the optimizer. Deriving the quadratic form of the performance index for the LQT has been proved in [29]. The benefit of quadratic forms is the availability of algorithms that can solve Bellman equations online. To cope with the reference trajectory, an augmented system is generated by incorporating the reference current

trajectory into the state space model of SRM. This augmented system leads to the development of ARE, which provides the optimal solution for the LQT. By solving ARE, the feedback and feedforward parts of the policy for the classic solution of the LQT are solved at the same time [30]. The main drawback of using the LQT Bellman equation to solve this problem is that the accurate model of SRM is required [31].

To cope with this issue, Q-learning is utilized to learn and adapt itself to the optimal solution of this LQT online. The LQT Bellman equation and Q-learning algorithm for the SRM drive system are introduced in this section.

A. THE LQT BELLMAN EQUATION ALGORITHM OF SRM DRIVE

A schematic diagram of a switched reluctance motor is depicted in Fig. 1, and Fig. 2 shows the circuit diagram of an SRM driver in a 3-phase and detailed single phase. Driving an SRM requires a train of current pulses applied with respect to the rotor position. Due to the negligible mutual inductance between phases and as done traditionally, the mutual inductances are neglected to achieve a phase model that is independent of other phases. Taking into consideration the reference current, an augmented system can be formed by discretizing the SRM model using the forward approximation as

$$X_{k+1} = \begin{bmatrix} A & 0 \\ 0 & F \end{bmatrix} \begin{bmatrix} x_k \\ r_k \end{bmatrix} + \begin{bmatrix} B \\ 0 \end{bmatrix} u_k \equiv A_a X_k + B_b u_k \quad (1)$$

$$Y_k = \begin{bmatrix} C & 0 \end{bmatrix} x_k \equiv C_c X_k \quad (2)$$

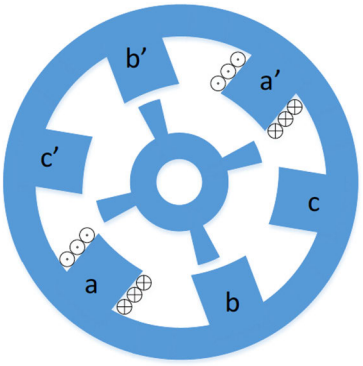

FIGURE 1. The schematic of an SRM.

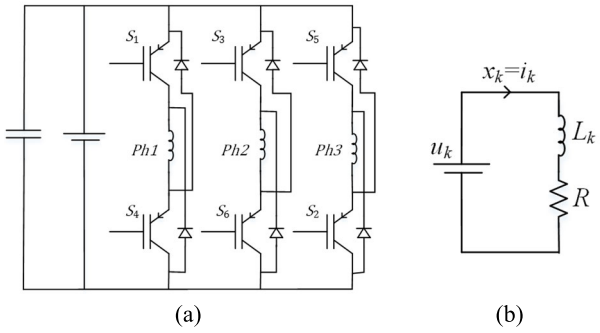

FIGURE 2. The circuit diagram of an SRM driver, (a) 3-phase drive circuit (b) single phase circuit diagram.

where $X_k = [x_k r_k]^T$ and $A = 1 - TR/L_k$, $B = T/L_k$, x_k is the phase current, u_k is the DC-bus voltage, R is the phase resistance, and the original output of the system y_k is the phase current, meaning that $C = 1$. The parameter L_k is the nonlinear phase inductance as a function of both phase current and rotor position. Parameter T is the sampling time and F is the model of the reference trajectory (i.e. $F = 1$ for a flat current). Due to the actual mechanical design of the machine, the nature of the inductance surface with respect to a rotor angle is periodic, starting from an unaligned position between rotor and stator poles until they are aligned. To solve the LQT problem and achieve tracking, the reference current generator pulses are assumed to be incorporated in the augmented system as in (1). It is expressed as

$$r_{k+1} = Fr_k \quad (3)$$

where r_k is the reference current trajectory and $F \in R^n$ is the reference current generator. This can generate different types of waveforms, including a sequence of square waveforms, the reference current for SRM. Even the command generator is not stable, then solving the LQT problem can occur by injecting the discount factor into the value function. Based on the augmented system, the discounted value function can be expressed as

$$V(x_k) = \frac{1}{2} \sum_{i=k}^{\infty} \gamma^{i-k} [X_i^T Q_q X_i + u_i^T R u_i] \quad (4)$$

where $Q_q = [C \ -I]^T Q [C \ -I]$, Q and R are predefined weight matrices for the augmented state and the control input, respectively, and $0 < \gamma \leq 1$ is a discount factor. It is important to consider that matrices Q and R are constant, positive-semi-definite and positive definite matrices, respectively. However, in the finite time horizon, they do not need to be constant. The value of γ should be less than 1 to attain a stable value function as the reference current in SRM is generated as a train of pulses and therefore has a positive dc average [32]. Based on (5), the value function relies on the current augmented state and an infinite horizon of the control inputs. By initializing the state of the value function with fixed control input, that infinite sum can be written as

$$V(x_k) = \frac{1}{2} \left[(r_k - y_k)^T Q (r_k - y_k) + u_k^T R u_k \right] + \gamma V(X_{k+1}) \quad (5)$$

Equation (4) is equivalent to the LQT bellman equation. As it has been proved in [29] that the value function can be derived in a quadratic form and $V(x_k) = \frac{1}{2} X_k^T P X_k$, the LQT Bellman equation with respect to a kernel P matrix is generated as

$$X_k^T P X_k = x_i^T Q_q x_i + u_k^T R u_k + \gamma X_{k+1}^T P X_{k+1} \quad (6)$$

where P matrix is the optimum solution of ARE with elements derived in [29]. By obtaining the Hamiltonian function of the LQT and applying the stationary condition to obtain the optimal control policy (8), the solution of ARE that allows the

matrix P to converge to its optimal values can be generated as

$$P = Q_q + \gamma A_a^T P A_a - \gamma^2 A_a^T P B_b (R + \gamma B_b^T P B_b)^{-1} B_b^T P A_a \quad (7)$$

Now, one may construct the algorithm based on the policy iteration method to solve the LQT problem by iterating the Bellman equation until convergence using data measured during the operation of the machine as in algorithm 1 as follows.

B. THE Q-LEARNING ALGORITHM OF SRM DRIVE

Let's assume that L_k and hence the model of the machine is linear. For instance, the controller is operating while the variations of the current and angle of the rotor are negligible. This is due to the fact that the Q-learning algorithm utilized in this section can only operate on linear systems. In the next section, the nonlinearity is addressed through scheduling.

In Algorithm 1, Policy Integration (PI) is applied to LQT Bellman equation to acquire the optimum solution for ARE.

This algorithm requires all SRM dynamic parameters (i.e. A_a) to solve the LQT problem online. Q-learning is among the RL control methods that offer an adaptive tuning algorithm to track the reference signal online without requiring the system dynamic [33]. By extracting sets of data during the operation, including the reference current and augmented states, the algorithm can train Q-function until convergence at each iteration. The Q-function of LQT can be provided in matrix form by substituting the augmented model (1) and reference current in the LQT Bellman equation as

$$Q(X_k, u_k) = \frac{1}{2} \begin{bmatrix} X_k \\ u_k \end{bmatrix}^T \begin{bmatrix} Q_q + \gamma A_a^T P A_a & \gamma A_a^T P B_b \\ \gamma B_b^T P A_a & R + \gamma B_b^T P B_b \end{bmatrix} \begin{bmatrix} X_k \\ u_k \end{bmatrix} \quad (8)$$

which can be written as

$$Q(X_k, u_k) = \frac{1}{2} \begin{bmatrix} X_k \\ u_k \end{bmatrix}^T \begin{bmatrix} G_{XX} & G_{Xu} \\ G_{uX} & G_{uu} \end{bmatrix} \begin{bmatrix} X_k \\ u_k \end{bmatrix} \quad (9)$$

The Q-learning algorithm can be designed based on the policy iteration method to solve the LQT online in a way that ensures the system model parameters do not appear in the algorithm processes [34]. This process improves the control input until the system converges to the optimal level, which allows the output current in the SRM to follow the reference current. Algorithm 2 demonstrates the procedure of finding the solution to the Q-learning. In this algorithm, M is defined as $M = [X_k \ u_k]^T$. Optimizing the Q-function in Algorithm 2 can be achieved as G matrix trains and converges to the optimum solution. The policy evaluation step for both algorithms 1 and 2 requires the solver to achieve convergence before updating the policy [31].

Algorithm 1 Solving LQT Bellman Equation Online by Using PI

Initialization: Initialize the algorithm with stable control input. Repeat and update the following two process until convergence.

1) Policy Evaluation:

$$X_k^T P^{i+1} X_k = (X_k^T) \left(Q_q + (K_P^i)^T R (K_P^i) \right) (X_k) + \gamma X_{k+1}^T P^{i+1} X_{k+1} \quad (10)$$

2) Policy Improvement:

$$K_P^{i+1} = (R + \gamma B_b^T P B_b)^{-1} \gamma B_b^T P A_a \quad (11)$$

Algorithm 2 Solving LQT Q-Function Online by Using PI

Initialization: Initialize the algorithm with stable control input. Repeat and update the following two process until convergence.

1) **Policy Evaluation:**

$$M_k^T G^{i+1} M_k = (X_k^T) Q_q (X_k) + (u_k^i)^T R (u_k)^i + \gamma M_{k+1}^T G^{i+1} M_{k+1} \quad (12)$$

2) **Policy Improvement:**

$$u_k^{i+1} = -(G_{uu}^{-1})^{i+1} G_{uX}^{i+1} X_k \quad (13)$$

III. Q-LEARNING SCHEDULING

In the previous section, the adaptive Q-learning algorithm controller for SRM was proposed to solve LQT and enable the current of the SRM drive to track a reference trajectory assuming that L_k was constant. The inductance profile of the SRM is a nonlinear function of the current and the rotor angle. For instance, the inductance profile of the motor utilized later in the experimental section is shown in Fig. 3. In addition to this function, in the long term, effects such as aging of bearings and changes in the airgap, chemical degradation of the core such as rust, which can lead to changes in the airgap length, and temperature expansion can cause further variation in the inductance profile. Also, common manufacturing related variations such as variations in the airgap length, permeability, and even number of turns can cause some differences between the expected model and the actual inductance profile. To mitigate these effects, adaptive estimation approaches to update the dynamic parameters of the machine are of interest. Various methods have been utilized to estimate the inductance profile of SRM and update the nonlinear model of the SRM [35], [36]. However, these methods are unlike the proposed Q-learning approach, which can perform both tracking reference and adaptive estimation at the same time. The Q-learning by itself is not feasible or applicable to a nonlinear system such as an SRM. To address this issue, one can incorporate a proper local linearization scheme for the nonlinear inductance surface of SRM to allow the Q matrix to train in its locally linearized region.

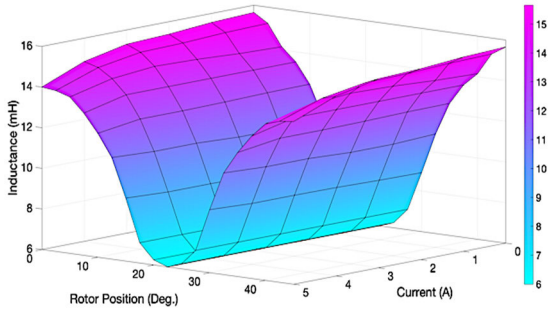

FIGURE 3. The inductance profile of the SRM used later during experimental testing with respect to the rotor angles and the currents.

Gain scheduling is a powerful solution to enable a linear control solution to address a nonlinear control problem. Gain scheduling is commonly applied to classical PID controllers to fine tune control parameters for the local operating conditions. Several implementations of gain scheduling methods have been studied for SRM control such as in speed control [37] and in PI current controller for enhancing the performance [38]. Gain scheduling allows the Q-learning algorithm to react rapidly to variations in operating conditions. For this, it is important to select enough Q-cores to reflect the nonlinear system properly. In contrast to nonlinear RL methods for adaptive dynamic programming such as neural networks which require heavy matrix operations for online training, gain scheduling provides fewer computation loads, which makes it ideal for implementations on conventional microcontrollers. Its major requirement is access to sufficient memory to store all trained Q matrix in the table elements based on the corresponding states and rotor angles. The data table must be updated for each iteration during system trajectories.

In this article, the surface of the inductance profile of SRMs is divided into sufficient segments to achieve a suitable linearization with a balanced tradeoff between the number of table elements and accuracy. Each Q-core represents a local linear controller that can follow the trajectory for that specific region of operation. The Q-learning algorithm can be executed in each segment by training a Q matrix in the segment until the matrix achieves its optimum solution based on the data collected from that segment. The training Q matrix at each segment is registered and stored as a table entry to generate a bidimensional Q matrix array which helps to efficiently conquer the nonlinear behavior of SRM.

For a fast control response, the Q-core table is fully trained using the expected parameters and then preloaded into the control system. This allows the controller to only adapt to the variations between the expected and actual model. The following subsections show the process of the Q-scheduling algorithm and its stages. The first stage involves solving and training Q-functions at each Q-core and can be performed using the least square method. The table implementation method will then transmit the scheduled Q matrix from the Q-table to the policy improvement to update the control input.

A. TRAINING LOCAL Q MATRICES

In this article, the least square approach has been utilized to solve the tracking problem and learn the Q matrix by using enough data packets measured through the operating of the machine. The least square solver does not require a system identification model. In practice, an observer is required to observe that states online. To implement policy evaluation, no less than $H = (m_x + m_u + m_y) \times (m_x + m_u + m_y + 1)/2$ data tuples are needed to perform LS method while $Q(X_k, u_k) = \frac{1}{2} M_k^T G M_k$ and the number of elements in G matrix are $(m_x+m_u+m_y)\times(m_x+m_u+m_y)$. This can be solved using the Kronecker product. The Kronecker product of $G_{m\times n}$ and $Z_{p\times q}$ can be defined as $G \otimes Z = \begin{bmatrix} g_{11} \cdot Z & \cdots & g_{1n} \cdot Z \\ \vdots & \ddots & \vdots \\ g_{m1} \cdot Z & \ldots & g_{mn} \cdot Z \end{bmatrix}$. Kronecker product enables the Q matrix to appear as columns of stacking vectors as

$$\mathcal{A}\left(vec(G)^T\right) = \mathcal{B} \tag{14}$$

The definition of A_k and B_k are expressed as

$$\mathcal{A} = \begin{bmatrix} M_k \otimes M_k - \gamma M_{k+1} \otimes M_{k+1} \\ \vdots \\ M_{k+z} \otimes M_{k+z} - \gamma M_{k+z+1} \otimes M_{k+z+1} \end{bmatrix} \tag{15}$$

$$\mathcal{B} = \begin{bmatrix} (X_k^T) Q_q(X_k) + (u_k^i)^T R (u_k)^i \\ \vdots \\ (X_{k+z}^T) Q_q(X_{k+z}) + (u_{k+z}^i)^T R (u_{k+z})^i \end{bmatrix} \tag{16}$$

where $z \geq H$ is the number of samples for each iteration. Then, the batch least square equation for solving Q matrix is provided as

$$vec\left(G^{j+1}\right) = (\mathcal{A}^T \mathcal{A})^{-1} \mathcal{A}^T \mathcal{B} \tag{17}$$

By maintaining the persistence condition, least square may be solved iteratively by applying recursive least square (RLS) equations as

$$e_k(t) = Q(X_k, u_k) - \mathcal{A}_k^T \overline{G}_k(t-1) \tag{18}$$

$$\overline{G}_k(t) = \overline{G}_k(t-1) + \frac{\eta_k(t-1)\mathcal{A}_k e_k}{1 + \mathcal{A}_k^T \eta_k(t-1)\mathcal{A}_k} \tag{19}$$

$$\eta_k(t) = \eta_k(t-1) - \frac{\eta_k(t-1)\mathcal{A}_k \mathcal{A}_k^T \eta_k(t-1)}{1 + \mathcal{A}_k^T \eta_k(t-1)\mathcal{A}_k} \tag{20}$$

where t is the index of iterations of the RLS, e is the error, and η is the covariance matrix whereas $\eta_k(0) = \tau I$ for a big positive number τ while I is an identity matrix.

B. TABLE DATA EXTRACTION AND LINEAR INTERPOLATION

Table readout algorithm is important to enabling extracting the knowledge from the Q-cores table and utilizing the data to improve policy. A table of Q-learning has been computed and formed in the previous section that contains the locations for current-rotor position points selected from the surface of the inductance profile. The typical current pulse for each SRM

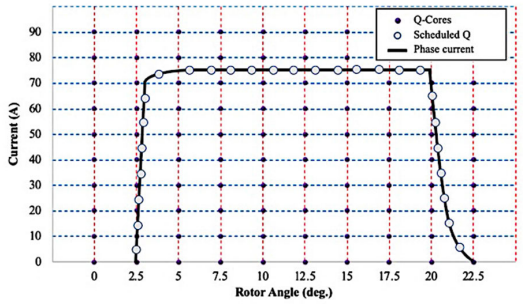

(a)

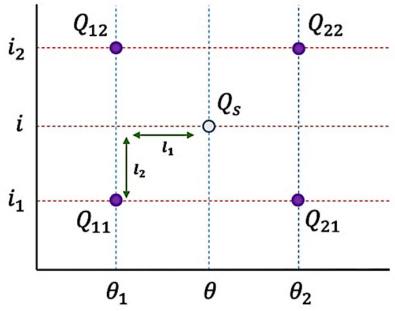

(b)

FIGURE 4. The process of implanting the Q-cores table into the controller, (a) The sample current path lies on the Q-cores table, (b) the definition of the bilinear scheduling parameters.

phase placed on the Q-learning table is shown in Fig. 4-a. One method of implementing the Q-learning table is to use the optimal Q matrix that is located at near the current path. In this case, the algorithm will read the value of the current and measure the distance to neighboring matrices to find the nearest Q matrix. This process solves the problem of using only one learned Q matrix in the locally linearized region. Although, in practice, this method is relatively simple, it leads to transients in the current waveform every time the controller switches between two table elements.

The bilinear interpolation algorithm provides a smoother and more accurate scheduling than does the nearest Q matrix method. This algorithm divides the Q matrix among its four closest Q matrices neighbors in the opposite proportion of the distance, which means if the state of the system is located at equal distance from four Q neighbors, the values of scheduled Q matrix are divided equally; if it is a near one of the four matrices, most of the scheduled Q matrix data are transmitted from that adjacent Q matrix. Observing the four neighboring Q matrices points Q_{11}, Q_{12}, Q_{21} and Q_{22}, which are the four closest neighbors of scheduled Q matrix Q_s, then Q_s is obtained as

$$Q_s = \beta_0 + \beta_1\theta + \beta_2 i + \beta_3\theta i \tag{21}$$

where the coefficient of bilinear scheduling β_0, β_1, β_2 and β_3 are obtained by solving

$$\begin{bmatrix}\beta_0\\ \beta_1\\ \beta_2\\ \beta_3\end{bmatrix} = \begin{bmatrix}1 & \theta_1 & i_1 & \theta_1 i_1\\ 1 & \theta_1 & i_2 & \theta_1 i_2\\ 1 & \theta_2 & i_1 & \theta_2 i_1\\ 1 & \theta_2 & i_2 & \theta_2 i_2\end{bmatrix}^{-1}\begin{bmatrix}Q_{11}\\ Q_{21}\\ Q_{12}\\ Q_{22}\end{bmatrix} \tag{22}$$

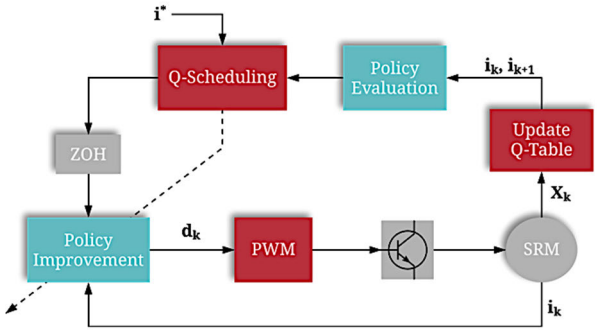

FIGURE 5. The overall control block diagram.

In practical implementation, to avoid solving systems of equations and performing matrix inversions that are not feasible in a digital controller, and since the scheduled Q matrix lies on a square grid of four Q matrices, one can use a simplified algorithm based on a unit square, Q_s is computed as

$$Q_s = \begin{bmatrix}1-l_2 & l_2\end{bmatrix}\begin{bmatrix}Q_{11} & Q_{12}\\ Q_{21} & Q_{22}\end{bmatrix}\begin{bmatrix}1-l_1\\ l_1\end{bmatrix} \tag{23}$$

where $l_1 \in [0, 1)$ and $l_2 \in [0, 1)$ are the lengths between Q_s and the nearest Q matrix in the rotor angels and current axis, respectively. These lengths are calculated as shown in Fig. 4-b as $l_1 = (\theta - \theta_1/\theta_2 - \theta_1)$ and $l_2 = (i - i_1/i_2 - i_1)$. Implementing this method drastically minimizes the computational burden of the scheduling process and the number of cycles required for scheduling.

IV. SIMULATION RESULTS

The Q-learning algorithm integrated with the bilinear scheduling approach has been simulated to study the performance of the proposed current controller and verify the effectiveness of the controller. The control scheme is depicted in Fig. 5. This controller has been applied to a 500 W 12/8 SRM, which has a phase resistance of 2 Ω and a nominal current of 5 A. The inductance profile of the controller begins from the aligned position at 16 mH and gradually decreases until it reaches the unaligned position at 6 mH. The available dc voltage is 100V. The simulation sampling time is defined by the switching frequency. In other words, for this simulation that the switching frequency is 10kHz, the sampling time is 1/10kHz equal to 0.1 millisecond. The control cycle in which the Q-learning/hysteresis performs is also defined by the switching frequency. To smoothen the simulation results, the time step for electrical parts 0.1 of the control cycle (10 microseconds). Algorithm 2 has been utilized for training all Q-cores pre-located on the nonlinear surface of the machine. In this case, the algorithm should initialize the process using a stable control policy and an augmented state. The initial augmented state and initial control policy have been selected to be $X_0 = [0\ 0]^T$ and $K_0 = [100\ -100]^T$, respectively. The cost function has been applied with the weights of

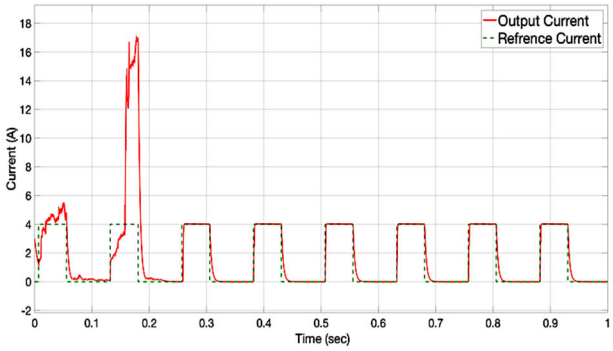

FIGURE 6. Tracking the output current of SRM to the reference current.

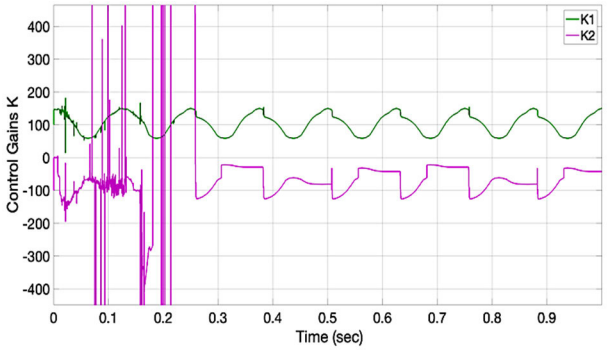

FIGURE 7. The convergence of the gains K values throughout learning process.

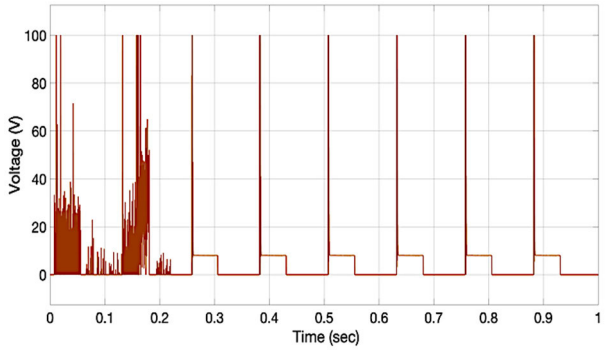

FIGURE 8. The optimal phase voltage introduced to the machine throughout learning.

Q = 100 and R = 0.001. The discount factor in this function is $\gamma = 0.9$.

The ratio between Q and R is essential for training the local Q matrix. If the value of R is large, an extremely high cost associated with the control input will occur, which prevents the linear quadratic tracker from tracking the reference. Moreover, if there is a huge Q/R ratio or R=0, the controller will track the reference in the first step due to a huge applied control input. This means that the duty cycles switch between two values, either 0% or 100%, which allow the controller to act as a delta-modulation controller that causes a remarkably high pulsation on the current. Therefore, selecting an effective Q/R ratio for tracking controller is of interest that permits the control input to vary freely as well as preventing the controller from tracking the reference from the first cycle. Hence, we have chosen the weights to be Q = 100 and R=0.001 as they are the best selection based on a design technique.

The reference model generates a train of square wave signals, the typical reference current for SRM. The Q-matrix at the unaligned position and a current of 4 A converges to its optimal values to allow tracking performance as shown below:

$$G = \begin{bmatrix} 438100 & -253100 & 5729 \\ -253100 & 56630 & -2595 \\ 5729 & -2595 & 98.1 \end{bmatrix} \quad (24)$$

And, the optimal control gain K converges to

$$K = \begin{bmatrix} 120 & -122 \end{bmatrix} \quad (25)$$

The optimal values vary based on Q-core along with the states that are located in the domain of the system. For each Q-core, there are 6 data tubules collected per iteration to train the Q-matrices using the LS method. In this simulation, the speed of the SRM is constant and has been selected to be 60 RPM to demonstrate the result for the proposed controller. Fig. 6 shows how the SRM drive current tracks the reference of sequent pulses within a few time steps. Fig. 7 shows how the control gains K values that have converged to their optimal numbers change (considering the movement along the scheduling-table as well). The optimal voltage signal introduced to the motor to verify the best tracking performance is shown in Fig. 8. Fig. 9 illustrates the behavior of the current once the reference changed from 4A to 5.5A. This figure depicts that the Q-table starts re-learning as a result of any change in the reference current. Hence, even though one cycle requires currents of up to 18A, the system will soon learn the correct model (in a practical application, over currents will be eliminated using a supervisory hysteresis band).

V. EXPERIMENTAL RESULTS

In this section, the results and observations are presented to show the practical feasibility of the control method. The experimental components include a 3-phase 500 W 12/8 SRM, DC machine with DC power supply to control the field and hence loading of the machine as a mechanical load, H bridge converter, control board with a TI TMS320F28377D microcontroller, and a mixed domain oscilloscope. The experimental setup is shown in Fig. 10. The unaligned and aligned inductances for the machine used for validation are 6mH and 16mH, respectively, and the nominal current is 5 A per phase. The proposed Q-learning algorithm is implemented inside one of the two TMS320F28377D cores capable of operating at 200MFLOPS each. The available processing power in this controller is sufficient to control a 3-phase SRM at a 40 kHz control frequency.

To demonstrate the effectiveness of the proposed Q-learning technique compared to the conventional hysteresis controller, both techniques are applied, where the proposed scheduled Q-learning approach controls the first

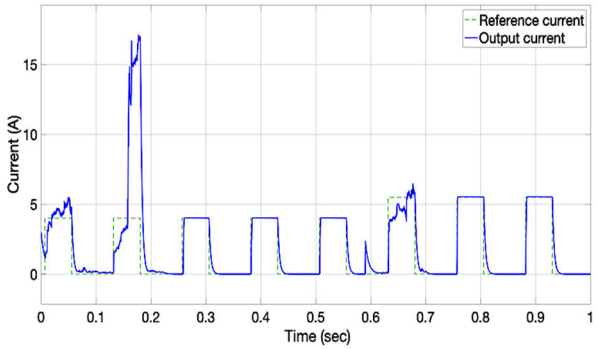

FIGURE 9. The behavior of current when the reference current changes.

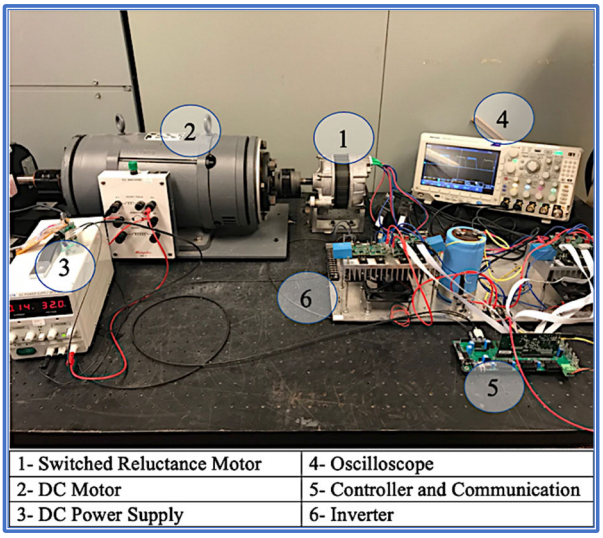

1- Switched Reluctance Motor	4- Oscilloscope
2- DC Motor	5- Controller and Communication
3- DC Power Supply	6- Inverter

FIGURE 10. The experimental setup.

phase, and the hysteresis technique controls the second and the third phase. The behavior of the current at different stages of the learning process is shown in Fig. 11. In this figure, the controller is set to run starting from the preloaded Q table to the point that the Q table is trained to the actual hardware online. In this figure, probe 1 shows the behavior of Phase A under the proposed control while probe 2 shows Phase B under the traditional Delta-modulation for comparison. During the learning process, when the Q matrices are not fully trained, the current tries to track the reference current (Fig. 11-a). The zoomed version of the current response is shown in Fig. 11-b. After a couple of cycles, the Q matrices are fully trained and the current can successfully track the reference current with almost no ripples on the current pulses (Fig. 11-c). Delta-modulation is not effective in minimizing the ripples for the current pulses. The Q-learning algorithm, once the Q-matrices are fully trained, are much more effective at minimizing the ripples for current pulses.

A. CHANGING THE REFERENCE CURRENT RESPONSE

In this test, the reference current is changed from 5.5 A to 4.5 A. The observations are illustrated in Fig. 12. This figure shows that the Q-matrices begin retraining once the

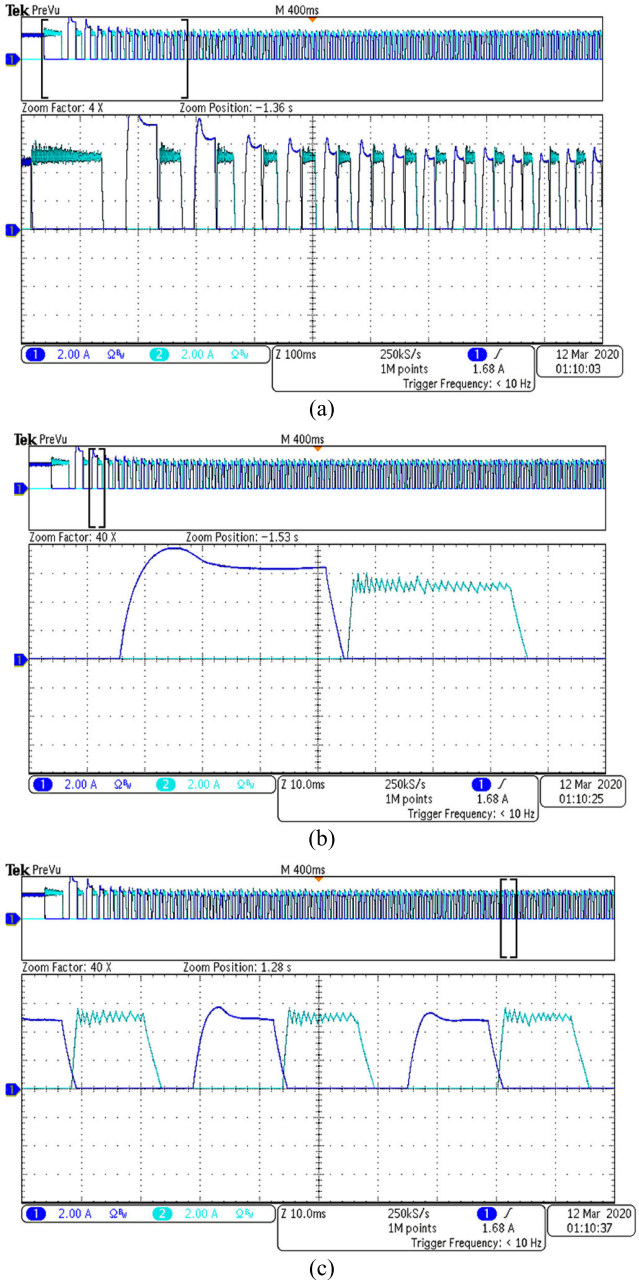

FIGURE 11. Startup process with the current set on 5.5 A (a) when the Q matrices are not fully trained, (b) the zoomed version of current response when the Q matrices are not fully trained (c) the current response when the Q matrix is fully trained.

reference current varies to 4.5 A. Fig. 12-a shows how the new reference is tracked. After a few cycles, the current tracks the reference effectively after the Q-matrices are fully trained (Fig. 12-b). When conventional delta-modulation is used, large ripples will be observed in phase current, and there is no way to mitigate them (Fig. 12-b).

To illustrate the novelty of the proposed technique, it can be seen that a model-free Q-learning control can regulate the current in only three cycles, which in general is less than 15 milliseconds. Moreover, the proposed technique reduces the ripples significantly compared to the conventional hysteresis

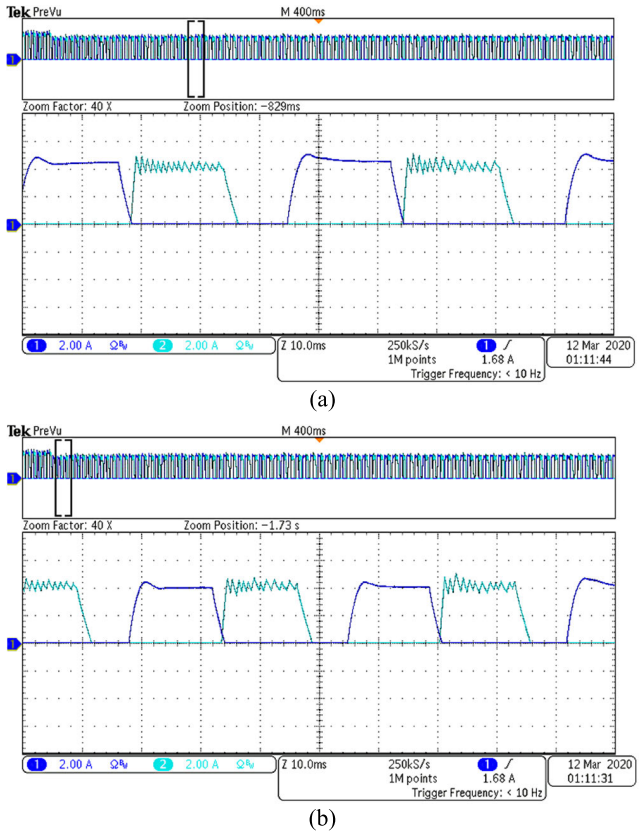

FIGURE 12. Reference change from 5.5 to 4.5A (a) when the Q matrices are not fully trained, (b) When the Q matrices are trained.

method. Finally, the controller does not need any tuning if the SRM parameters changes because aging or change in airgaps, since the online training never stops learning. In this article, the proposed Q-learning parameters are only the discount factor and the size of the Q-table. These parameters are defined based on the trial-and-error technique.

B. HARDWARE IMPLEMENTATION CHALLENGES

Laboratory testbeds always arise new challenges compared to the simulation. Computationally feasibility is the main obstacle of the experimental testbeds, which includes two main parts: (i) whether the controller can be implemented easily? For instance, regarding the reinforcement learning methods, there are several functions, libraries, and toolboxes available in MATLAB and Python that can facilitate the implementation, that are not available in embedded compilers. The main advantage of the proposed technique is its easy-to-implement characteristics. The iterative inherence of the proposed technique limits the mathematical operation to summations, multiplications, and square roots. The embedded TI microcontroller, TMS320F28377D, includes embedded hardware multiplier and square root blocks, which significantly decreases the computation time. (ii) if the controller can fit in the control cycle. In this article, where the controller only requires a few numbers of multiplications and summation, a 200 MHz microcontroller can easily implement the algorithm. However, for more complicated reinforcement learning methods with multilayer neural network, forward computations, and back propagation training, alternative solutions are required, which are not the main concern of this article.

VI. CONCLUSION

The Q-learning scheduling algorithm for controlling the current of an SRM drive was studied in this article. By defining a Q-learning LQT, a table of Q-cores was generated to cover the nonlinear surface of the SRM model. Using this table, a scheduled Q-learning controller was derived, which is capable of controlling a nonlinear system, particularly, an SRM drive. Additionally, an online training mechanism was introduced capable of controlling the SRM without having any information regarding the system model parameters. This training mechanism updates each Q-core in the table as the state variables evolve over the domain of this table. Furthermore, a linear interpolation technique was used to ensure smooth transitions between these Q-cores. Lastly, simulation and experimental results demonstrated that the proposed algorithm is successful in controlling the current of a switched reluctance motor, minimizing its ripples, and adapting to the underlying SRM without any prior information regarding its parameters.

REFERENCES

[1] N. Yan, X. Cao, and Z. Deng, "Direct torque control for switched reluctance motor to obtain high Torque–Ampere ratio," *IEEE Trans. Ind. Electron.*, vol. 66, no. 7, pp. 5144–5152, Jul. 2019, doi: 10.1109/TIE.2018.2870355.

[2] Q. Sun, J. Wu, C. Gan, C. Shi, and J. Guo, "DSSRM design with multiple pole arcs optimization for high torque and low torque ripple applications," *IEEE Access*, vol. 6, pp. 27166–27175, 2018, doi: 10.1109/ACCESS.2018.2834901.

[3] M. Kawa, K. Kiyota, J. Furqani, and A. Chiba, "Acoustic noise reduction of a high-efficiency switched reluctance motor for hybrid electric vehicles with novel current waveform," *IEEE Trans. Ind. Appl.*, vol. 55, no. 3, pp. 2519–2528, May 2019, doi: 10.1109/TIA.2018.2888847.

[4] V. Valdivia, R. Todd, F. J. Bryan, A. Barrado, A. Lázaro, and A. J. Forsyth, "Behavioral modeling of a switched reluctance generator for aircraft power systems," *IEEE Trans. Ind. Electron.*, vol. 61, no. 6, pp. 2690–2699, Jun. 2014, doi: 10.1109/TIE.2013.2276768.

[5] H. Chen, W. Yan, J. J. Gu, and M. Sun, "Multiobjective optimization design of a switched reluctance motor for low-speed electric vehicles with a Taguchi–CSO algorithm," *IEEE/ASME Trans. Mechatronics*, vol. 23, no. 4, pp. 1762–1774, Aug. 2018, doi: 10.1109/TMECH.2018.2839619.

[6] K. Kiyota and A. Chiba, "Design of switched reluctance motor competitive to 60-kW IPMSM in third-generation hybrid electric vehicle," *IEEE Trans. Ind. Appl.*, vol. 48, no. 6, pp. 2303–2309, Nov. 2012, doi: 10.1109/TIA.2012.2227091.

[7] M. Krishnamurthy, C. S. Edrington, A. Emadi, P. Asadi, M. Ehsani, and B. Fahimi, "Making the case for applications of switched reluctance motor technology in automotive products," *IEEE Trans. Power Electron.*, vol. 21, no. 3, pp. 659–675, May 2006, doi: 10.1109/TPEL.2006.872371.

[8] P. Shamsi and B. Fahimi, "Single-bus star-connected switched reluctance drive," *IEEE Trans. Power Electron.*, vol. 28, no. 12, pp. 5578–5587, Dec. 2013, doi: 10.1109/TPEL.2013.2251475.

[9] Y. Yang, N. Schofield, and A. Emadi, "Double-rotor switched reluctance machine (DRSRM)," *IEEE Trans. Energy Convers.*, vol. 30, no. 2, pp. 671–680, Jun. 2015, doi: 10.1109/TEC.2014.2378211.

[10] W. Wang, M. Luo, E. Cosoroaba, B. Fahimi, and M. Kiani, "Rotor shape investigation and optimization of double stator switched reluctance machine," *IEEE Trans. Magn.*, vol. 51, no. 3, Mar. 2015, Art. no. 8103304, doi: 10.1109/TMAG.2014.2356573.

[11] A. H. Isfahani and B. Fahimi, "Comparison of mechanical vibration between a double-stator switched reluctance machine and a conventional switched reluctance machine," *IEEE Trans. Magn.*, vol. 50, no. 2, pp. 293–296, Feb. 2014, doi: 10.1109/TMAG.2013.2286569.

[12] R. Gobbi and K. Ramar, "Optimisation techniques for a hysteresis current controller to minimise torque ripple in switched reluctance motors," *IET Electr. Power Appl.*, vol. 3, no. 5, pp. 453–460, Sep. 2009, doi: 10.1049/iet-epa.2008.0191.

[13] B. Shao and A. Emadi, "A digital PWM control for switched reluctance motor drives," in *Proc. IEEE Vehicle Power Propuls. Conf.*, Sep. 2010, pp. 1–6, doi: 10.1109/VPPC.2010.5729103.

[14] S. E. Schulz and K. M. Rahman, "High-performance digital pi current regulator for ev switched reluctance motor drives," *IEEE Trans. Ind. Appl.*, vol. 39, no. 4, pp. 1118–1126, Jul. 2003, doi: 10.1109/TIA.2003.814580.

[15] F. Blaabjerg, P. C. Kjaer, P. O. Rasmussen, and C. Cossar, "Improved digital current control methods in switched reluctance motor drives," *IEEE Trans. Power Electron.*, vol. 14, no. 3, pp. 563–572, May 1999, doi: 10.1109/63.761700.

[16] J. Ye, P. Malysz, and A. Emadi, "A fixed-switching-frequency integral sliding mode current controller for switched reluctance motor drives," *IEEE J. Emerg. Sel. Topics Power Electron.*, vol. 3, no. 2, pp. 381–394, Jun. 2015, doi: 10.1109/JESTPE.2014.2357717.

[17] S. M. Lukic and A. Emadi, "State-switching control technique for switched reluctance motor drives: Theory and implementation," *IEEE Trans. Ind. Electron.*, vol. 57, no. 9, pp. 2932–2938, Sep. 2010, doi: 10.1109/TIE.2009.2038942.

[18] M. Ali Akcayol, "Application of adaptive neuro-fuzzy controller for SRM," *Adv. Eng. Softw.*, vol. 35, nos. 3–4, pp. 129–137, Mar. 2004, doi: 10.1016/j.advengsoft.2004.03.005.

[19] X. Li and P. Shamsi, "Model predictive current control of switched reluctance motors with inductance auto-calibration," *IEEE Trans. Ind. Electron.*, vol. 63, no. 6, pp. 3934–3941, Jun. 2016, doi: 10.1109/TIE.2015.2497301.

[20] R. Mikail, I. Husain, Y. Sozer, M. S. Islam, and T. Sebastian, "A fixed switching frequency predictive current control method for switched reluctance machines," *IEEE Trans. Ind. Appl.*, vol. 50, no. 6, pp. 3717–3726, Nov. 2014, doi: 10.1109/TIA.2014.2322144.

[21] S. S. Ahmad and G. Narayanan, "Predictive control based constant current injection scheme for characterization of switched reluctance machine," *IEEE Trans. Ind. Appl.*, vol. 54, no. 4, pp. 3383–3392, Jul. 2018, doi: 10.1109/TIA.2018.2818646.

[22] Z. Lin, D. Reay, B. Williams, and X. He, "High-performance current control for switched reluctance motors based on on-line estimated parameters," *IET Electr. Power Appl.*, vol. 4, no. 1, pp. 67–74, Jan. 2010, doi: 10.1049/iet-epa.2009.0016.

[23] S. Saadatmand, S. Azizi, M. Kavousi, and D. Wunsch, "Autonomous control of a line follower robot using a Q-learning controller," in *Proc. 10th Annu. Comput. Commun. Workshop Conf. (CCWC)*, Jan. 2020, pp. 556–561, doi: 10.1109/CCWC47524.2020.9031160.

[24] X. Li and P. Shamsi, "Inductance surface learning for model predictive current control of switched reluctance motors," *IEEE Trans. Transport. Electrific.*, vol. 1, no. 3, pp. 287–297, Oct. 2015, doi: 10.1109/TTE.2015.2468178.

[25] P. J. Werbos, "Approximate dynamic programming for real-time control and neural modeling," in *Handbook of Intelligent Control*, D. A. White and D. A. Sofge, Eds. New York, NY, USA: Reinhold, 1992.

[26] S. He, M. Zhang, H. Fang, F. Liu, X. Luan, and Z. Ding, "Reinforcement learning and adaptive optimization of a class of Markov jump systems with completely unknown dynamic information," *Neural Comput. Appl.*, vol. 32, no. 18, pp. 14311–14320, Sep. 2020, doi: 10.1007/s00521-019-04180-2.

[27] S. He, H. Fang, M. Zhang, F. Liu, X. Luan, and Z. Ding, "Online policy iterative-based H_∞ optimization algorithm for a class of nonlinear systems," *Inf. Sci.*, vol. 495, pp. 1–13, Aug. 2019, doi: 10.1016/j.ins.2019.04.027.

[28] F. L. Lewis, D. L. Vrabie, and V. L. Syrmos, *Optimal Control*, 3rd ed. Hoboken, NJ, USA: Wiley, 2012.

[29] B. Kiumarsi, F. L. Lewis, H. Modares, A. Karimpour, and M.-B. Naghibi-Sistani, "Reinforcement -learning for optimal tracking control of linear discrete-time systems with unknown dynamics," *Automatica*, vol. 50, no. 4, pp. 1167–1175, Apr. 2014, doi: 10.1016/j.automatica.2014.02.015.

[30] B. Kiumarsi-Khomartash, F. L. Lewis, M.-B. Naghibi-Sistani, and A. Karimpour, "Optimal tracking control for linear discrete-time systems using reinforcement learning," in *Proc. 52nd IEEE Conf. Decis. Control*, Dec. 2013, pp. 3845–3850, doi: 10.1109/CDC.2013.6760476.

[31] F. L. Lewis and D. Vrabie, "Reinforcement learning and adaptive dynamic programming for feedback control," *IEEE Circuits Syst. Mag.*, vol. 9, no. 3, pp. 32–50, Dec. 2009, doi: 10.1109/MCAS.2009.933854.

[32] F. L. Lewis, D. Vrabie, and K. G. Vamvoudakis, "Reinforcement learning and feedback control: Using natural decision methods to design optimal adaptive controllers," *IEEE Control Syst.*, vol. 32, no. 6, pp. 76–105, Dec. 2012, doi: 10.1109/MCS.2012.2214134.

[33] A. Al-Tamimi, F. L. Lewis, and M. Abu-Khalaf, "Model-free Q-learning designs for linear discrete-time zero-sum games with application to H_∞ control," *Automatica*, vol. 43, no. 3, pp. 473–481, Mar. 2007, doi: 10.1016/j.automatica.2006.09.019.

[34] M. Abu-Khalaf, F. L. Lewis, and J. Huang, "Policy iterations on the Hamilton–Jacobi–Isaacs equation for H_∞ state feedback control with input saturation," *IEEE Trans. Autom. Control*, vol. 51, no. 12, pp. 1989–1995, Dec. 2006, doi: 10.1109/TAC.2006.884959.

[35] S. Song, M. Zhang, and L. Ge, "A new fast method for obtaining flux-linkage characteristics of SRM," *IEEE Trans. Ind. Electron.*, vol. 62, no. 7, pp. 4105–4117, Jul. 2015, doi: 10.1109/TIE.2015.2390147.

[36] K. Kiyota, T. Kakishima, and A. Chiba, "Comparison of test result and design stage prediction of switched reluctance motor competitive with 60-kW rare-Earth PM motor," *IEEE Trans. Ind. Electron.*, vol. 61, no. 10, pp. 5712–5721, Oct. 2014, doi: 10.1109/TIE.2014.2304705.

[37] W. K. Ho, S. K. Panda, K. W. Lim, and F. S. Huang, "Gain-scheduling control of the switched reluctance motor," *Control Eng. Pract.*, vol. 6, no. 2, pp. 181–189, Feb. 1998, doi: 10.1016/S0967-0661(98)00012-4.

[38] H. Hannoun, M. Hilairet, and C. Marchand, "Gain-scheduling PI current controller for a switched reluctance motor," in *Proc. IEEE Int. Symp. Ind. Electron.*, Jun. 2007, pp. 1177–1182, doi: 10.1109/ISIE.2007.4374765.

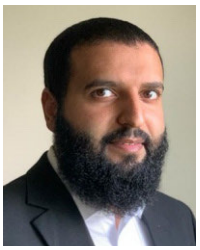

HAMAD ALHARKAN (Student Member, IEEE) received the B.Sc. degree in electrical engineering from Qassim University, Saudi Arabia, in 2011, and the M.Sc. degree in electrical engineering from the Missouri University of Science and Technology, USA, in 2016, where he is currently pursuing the Ph.D. degree. In 2013, he joined the Department of Electrical Engineering, College of Engineering, Qassim University, Unaizah, Saudi Arabia, as a Faculty Member. His research interests include microgrids, motor drive, and machine learning.

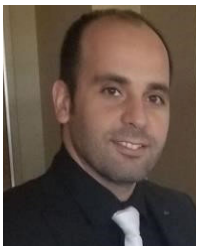

SEPEHR SAADATMAND (Student Member, IEEE) received the B.Sc. degree in electrical engineering from the Amirkabir University of Technology, Tehran, Iran, in 2008, the first M.Sc. degree in electrical engineering from the University of Tehran, Tehran, Iran, in 2011, and the second M.Sc. degree in electrical and computer engineering from Southern Illinois University, Carbondale, USA, in 2018. He is currently pursuing the Ph.D. degree in electrical engineering with the Missouri University of Science and Technology (formerly UMR), Rolla, MO, USA.

His research interests include power electronics, microgrids, motor drive, and machine learning application in power electronics.

MEHDI FERDOWSI (Member, IEEE) received the B.S. degree in electronics from the University of Tehran, Tehran, Iran, in 1996, the M.S. degree in electronics from the Sharif University of Technology, Tehran, in 1999, and the Ph.D. degree in electrical engineering from the Illinois Institute of Technology, Chicago, IL, USA, in 2004.

In 2004, he joined the Missouri University of Science and Technology, Rolla, MO, USA, as a Faculty, where he is currently a Professor with the Electrical and Computer Engineering Department. His research interests include power electronics, energy storage, smart grid, vehicular technology, and wide bandgap devices.

Dr. Ferdowsi was a recipient of the National Science Foundation CAREER Award, in 2007. He is an Associate Editor of the IEEE TRANSACTIONS ON POWER ELECTRONICS.

POURYA SHAMSI (Senior Member, IEEE) received the B.Sc. degree in electrical engineering from the University of Tehran, Tehran, Iran, in 2007, and the Ph.D. degree in electrical engineering from The University of Texas at Dallas, Richardson, TX, USA, in 2012.

He is currently the Woodard Associate Professor of electrical engineering with the Missouri University of Science and Technology (formerly UMR), Rolla, MO, USA. His research interests are power electronics, microgrids, reachability of hybrid systems, networked control systems, and motor drives.